Crystal Growth

DOI: 10.1002/ange.200601871

Bioenabled Synthesis of Rutile (TiO_2) at Ambient Temperature and Neutral pH**

Nils Kröger, Matthew B. Dickerson, Gul Ahmad, Ye Cai, Michael S. Haluska, Kenneth H. Sandhage, Nicole Poulsen, and Vonda C. Sheppard*

Biomineralizing organisms are unmatched in their ability to form micro- to nanoscale hierarchically structured 3D inorganic materials under ambient conditions. Although the genetic foundations of the species-specific 3D architectures of biominerals are not well understood, specific organic molecules (mostly proteins) are known to guide their deposition and morphogenesis.[1–3] It has been suggested that the molecules and mechanisms of biomineralization may provide new paradigms for the environmentally benign syntheses of advanced nanopatterned materials.[4–6] Indeed, pioneering work by Morse and co-workers demonstrated that proteins (named silicateins) involved in the biomineralization of sponge silica spicules are able to catalyze in vitro the formation of silica and amorphous or partially crystallized, non-biological inorganic materials (titanium dioxide, titanium phosphates, gallium oxohydride, and gallium oxide).[7–12] Also, the hydrolytic enzyme lysozyme has been shown to induce formation of amorphous titania and silica.[13,14]

A different family of silica-forming proteins (named silaffins) has been characterized from diatoms, which are a group of unicellular microalgae (phytoplankton) that form intricately structured 3D silica microshells. Silaffins represent a unique family of phosphoproteins that share no sequence homology with sponge silicateins and exhibit a different mechanism of silica formation.[15a–c] Recently, poly(allylamine)[16a] and the synthetic non-phosphorylated 19-mer peptide R5, which corresponds to a repeat sequence of the silaffin

[*] Prof. Dr. N. Kröger, Dr. N. Poulsen, V. C. Sheppard
School of Chemistry and Biochemistry
Georgia Institute of Technology
770 State Street, Atlanta, GA 30332-0400 (USA)
Fax: (+1) 404-894-7452
E-mail: nils.kroger@chemistry.gatech.edu
M. B. Dickerson, Dr. G. Ahmad, Dr. Y. Cai, Dr. M. S. Haluska, Prof. Dr. K. H. Sandhage
School of Materials Science and Engineering
Georgia Institute of Technology
771 Ferst Drive, Atlanta, GA 30332-0245 (USA)

[**] This work was supported by the Office of Naval Research, the Air Force Office of Scientific Research, the Georgia Tech Research Corporation, and the Colleges of Science and Engineering of the Georgia Institute of Technology. We thank Matije Crne and Mohan Srinivasarao for help with polarized light microscopy. The authors acknowledge the FIB2 Center at Georgia Tech established under NSF, CRIF project number: 0343028.

Supporting information for this article is available on the WWW under http://www.angewandte.org or from the author.

precursor polypeptide sil1p, have been employed for silica and titania syntheses.[16b–d]

Despite these achievements, only amorphous or partially nanocrystalline minerals have been produced to date through in vitro mineralization, and the formation of hierarchical structures—a hallmark of biominerals—has not been achieved. It is reasonable to assume that silaffin proteins may exhibit improved mineral-forming activities, as compared with short peptides (such as the R5 peptide), owing to possible cooperative effects between the mineral-interacting protein domains. To investigate this possibility, selected regions of silaffin genes were expressed in *Escherichia coli* and purified to homogeneity (see Supporting Information). Their mineral-forming activities were then analyzed. The characteristic properties of recombinant silaffins rSilC, rSil1L, rSil3, and rSilN are listed in Table 1. Analyses by mass spectroscopy confirmed that the amino acid side chains of recombinant silaffins carry no post-translational modifications (data not shown).

Table 1: Properties of recombinant silaffins.[a]

	rSilC	rSil1L	rSil3	rSilN
M_{theor} [kDa]	17.6	11.8	22.1	9.9
pI	11.8	10.6	9.4	3.8
K + R	45 (27%)	15 (14%)	33 (16%)	2 (2%)
D + E	0	4 (4%)	30 (14%)	23 (27%)

[a] The theoretical molecular masses of the unmodified polypeptides are listed. pI = isolectric point. K + R = content of lysine and arginine residues, respectively. D + E = content of aspartate and glutamate residues, respectively.

Initial experiments were conducted to determine whether recombinant silaffins retained silica-formation activity. The silaffins rSilC, rSil1L, and rSil3 induced the precipitation of silica in the pH range 6–10, whereas no silica was deposited within the assay time (10 min) in the presence of rSilN or in the absence of silaffins. The complete amount of silaffin added to the silicic acid solution was incorporated into the precipitates, and the amount of silica produced increased linearly with the amount of recombinant silaffin added to the silicic acid solution. The silica precipitates were composed of aggregates of spherical particles that exhibited different sizes depending on the recombinant silaffin used (rSilC: 200–400 nm; rSil3: 50–250 nm; rSil1L: <50 nm; see Supporting Information). These morphologies were similar to the silica precipitates formed previously by polycationic peptides and proteins (e.g. R5 peptide, poly-L-lysine, lysozyme), which is consistent with a common mineralization mechanism. The proposed mechanism involves the flocculation of polysilicic acid particles (that form rapidly at pH ≥ 6) by polycationic peptide/protein molecules.[17–19]

It was then investigated whether recombinant silaffins were also able to induce the formation of TiO_2 (titania). Titania-based materials have a wide variety of applications in (photo)catalysis, gas sensing, and photovoltaics, and are used as pigments and phosphors.[20,21] The twofold negatively charged complex titanium(IV) bis-(ammonium lactato)-dihydroxide (TiBALDH) was used as a substrate for titania formation in buffered aqueous solutions. In the absence of silaffins, the solutions remained clear and homogenous for several hours, as did the solutions containing rSil3 and rSilN. However, when rSilC or rSil1L were added, the TiBALDH solutions instantly became turbid, and precipitates were formed after only a few minutes under all pH conditions tested (pH 3–10). Energy-dispersive X-ray (EDX) analyses yielded strong signals for Ti and O in the rSilC- and rSil1L-induced precipitates, indicating the presence of titania (see Supporting Information). The precipitates also contained the complete amount of recombinant silaffin added to the TiBALDH solutions (see Supporting Information). Thermogravimetric analyses (TGA) indicated an organic content of 56 wt% for rSilC–titania and 50 wt% for rSil1L–titania.

The rSil1L–titania was composed of large aggregates of randomly arranged nanospheres (diameters of 100–300 nm) that were partially fused together to form an interconnected network of particles (Figure 1a). The rSilC–titania contained two different types of structures (Figure 1b). One type consisted of aggregates of round particles (diameters of

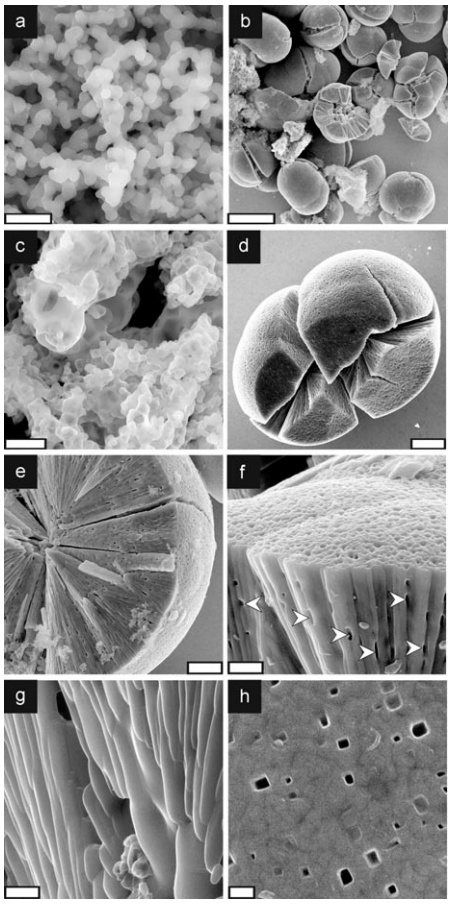

Figure 1. Titania formation by recombinant silaffins. a) SEM images of the precipitates formed by 53 μM rSil1L, and b–h) 32 μM rSilC in sodium phosphate/citrate buffer solution (50 mM; pH 7). The images in parts e–h were taken from fractured hemispheres. e) Part of the fractured hemisphere. f) Detail from the region near the external surface region; the arrowheads indicate some of the pores inside the microspheres. g) Detail of the central core region. h) Detail of the external surface. Scale bars: 20 μm (b), 5 μm (d, e), 1 μm (a, c, f), and 500 nm (g, h).

100 nm–1 μm) that were interconnected and, in many cases, appeared to be partially collapsed, which suggested that they were hollow (Figure 1c). This was indeed confirmed by scanning electron microscopy (SEM) analysis of focused ion beam (FIB) milled cross sections (see Supporting Information) as well as by transmission electron microscopy (TEM; see below). The second type of rSilC–titania structure consisted of large microspheres (diameters 20–50 μm) that were frequently cracked and/or fragmented (Figure 1b,d,e). Higher-magnification images revealed a remarkable hierarchical architecture (Figure 1e–h). The microspheres were comprised of radially arranged, densely packed columns of tapered cross-section. The columns revealed thicknesses of 400–800 nm on the larger ends (i.e. at the external surface; Figure 1f) and 100–200 nm on the smaller ends (i.e. at the central core; Figure 1g). Both on the external surfaces, and throughout the cross-sections of the microspheres, numerous rectangular pores with long edge lengths between 100–200 nm were observed (Figure 1f,h).

Selected-area electron diffraction (SAED) analyses of the columnar subunits of the microspheres yielded well-defined diffraction spots that could all be assigned to lattice planes of the titania polymorph rutile (Figure 2a,b). High-resolution (HR) TEM confirmed this result by revealing exclusively crystalline regions with a lattice spacing characteristic for (110) rutile (Figure 2c). In contrast, the aggregates of hollow particles (i.e. the second type of structure present in the rSilC–titania precipitate) were composed of an amorphous titania matrix containing a dispersion of anatase nanocrystals (Figure 2d–f).

Powder X-ray diffraction (XRD) analysis of rSilC–titania yielded diffraction peaks only for rutile (Figure 2g), presumably because the anatase nanocrystals (Figure 2f) were so low in abundance that they escaped detection. The XRD pattern obtained from the rSil1L–titania precipitate revealed broad diffraction peaks of low intensity, which were consistent with nanocrystals of a monoclinic titania polymorph (TiO_2–B)[22] (see Supporting Information).

The presence of oriented rutile microcrystals in the rSilC–titania precipitate is highly surprising. Conventional syntheses of microcrystalline rutile require high temperatures (e.g. 600–800 °C), and the formation of nanocrystalline rutile has so far only been achieved at extremely acidic pH values ($pH < 1$) and elevated temperatures.[23–36]

To further study the rSilC-induced formation of rutile microspheres, the process was followed by polarized light microscopy. The addition of rSilC to the aqueous TiBALDH solution rapidly induced formation of large, irregularly shaped aggregates (Figure 3a), which were consistent with the aggregates of round hollow particles observed by SEM analysis (see Figure 1c). These partially amorphous, partially crystalline particles (see Figure 2f) represented the end product in aqueous solution, even after prolonged incubation times (up to 24 h). In contrast, removal of the mother liquor 10 minutes after precipitation and subsequent dehydration—either by incubation in methanol or drying for 30 minutes in vacuo—induced the formation of rutile microspheres (Figure 3b,c). After extended periods of drying (≥ 24 h), the relative abundance of the irregularly shaped particle aggregates was strongly reduced, and crystalline microspheres were almost exclusively observed (Figure 3d).

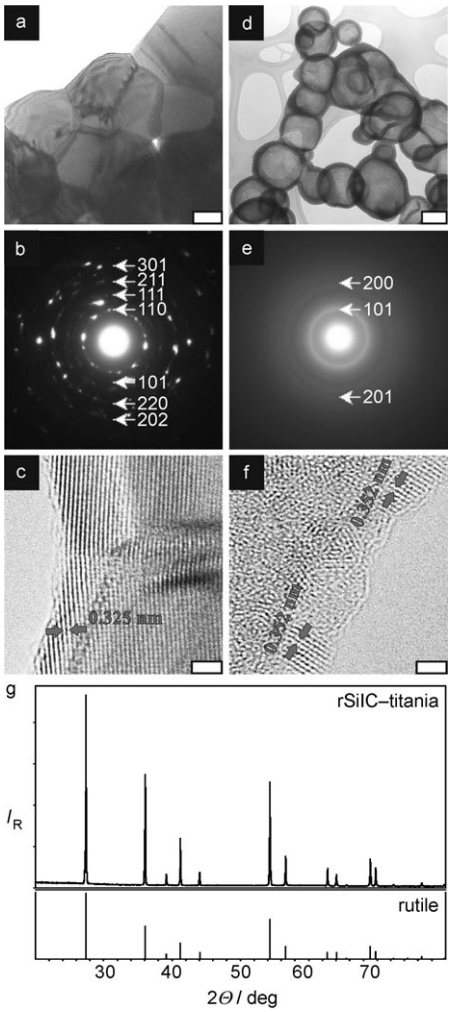

Figure 2. Structural analyses of rSilC–titania. TEM images obtained from microspheres (a) and the aggregates of hollow particles (d). SAED analyses obtained from a microsphere (b) and the shell of a hollow particle (e). Diffraction rings corresponding to rutile (b) and anatase (e) are assigned. HR-TEM analysis of a microsphere fragment showing the (110) lattice fringes of rutile (c, arrows), and from the shell region of a hollow particle showing the (101) lattice fringes of anatase (f, arrows). g) Powder X-ray diffraction analysis obtained from the rSilC–titania precipitate (I_R = relative intensity). Scale bars: 100 nm (a), 200 nm (d), 2 nm (c,f).

The transformation process from partially amorphous titania aggregates into highly organized rutile microspheres requires the reorganization of the condensed TiO_6 octahedra. This can usually only be achieved at high temperatures or under extremely acidic conditions.[23–36] We hypothesize that the rSilC molecules entrapped within the hydrated, partially amorphous titania mediate rutile crystallization by 1) acting as an acid–base catalyst in the hydrolysis and condensation reactions between TiO_6 octahedra, and 2) guiding the rearrangement of these units into a crystal lattice. The molecular characteristics of rSilC are well suited for these functions. The numerous lysine residues can donate and accept protons, and the highly repetitive spacing of functional groups in rSilC (see

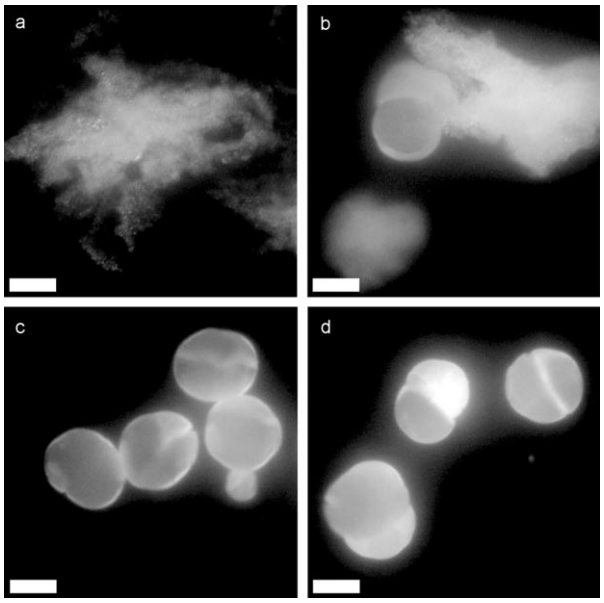

Figure 3. Analysis of microsphere formation by polarized light microscopy. The structures of rSilC–titania were documented at different processing stages: a) In mother liquor after 10-min reaction time; b) after subsequent washing with H_2O and methanol; c) after washing (with H_2O and methanol) and drying for 30 min in vacuo; and d) after continued drying for 24 h in vacuo. Scale bars: 20 μm.

Supporting Information) may lower the activation energy for the alignment of TiO_6 octahedra into a rutile lattice. In contrast, rSil1L, which is unable to induce rutile formation, contains only a short repetitive sequence region with less conserved repeated units (see Supporting Information). The synthetic homopolypeptide poly-L-lysine ($M_w = 15$–30 kDa) is also incapable of directing the formation of rutile and led rather to the deposition of anatase titania as the predominant crystalline phase (see Supporting Information). This indicates that the distribution of positive charges, the amino acid sequence/composition, the 3D polypeptide conformation, or a combination of these factors is crucial for rSilC's ability to induce rutile formation. The influence of these factors can be experimentally tested by site-directed mutagenesis of the rSilC polypeptide sequences.

The transformation of amorphous mineral deposits into crystalline phases has also been observed in biological mineralization processes. Many $CaCO_3$-forming organisms employ specific proteins to deposit structures made of amorphous $CaCO_3$, which in later stages crystallize as calcite.[37] By using a system in vitro that is based on self-assembled monolayers, Aizenberg et al. have mimicked this strategy and demonstrated that the transformation of amorphous $CaCO_3$ into calcite required sufficient removal of the H_2O associated with the amorphous phase. This was achieved by introducing closely spaced channels into which the H_2O was expelled during the crystallization process.[38] As shown in the present study, the removal of H_2O is also critical for the rSilC-induced transformation of the hydrated, partially amorphous titania aggregates into rutile microspheres (see Figure 3). It is suggested that the numerous pores present within the rutile microspheres (Figure 1 f,h) may act as H_2O release channels that enable the crystallization process to occur. The mechanism of pore formation within the rutile microspheres is currently unclear.

The ability of recombinant silaffin rSilC to induce the formation of rutile under ambient conditions and neutral pH is unprecedented, and opens up new possibilities to produce functional hybrid materials for optical applications.

Experimental Section

Selected regions of silaffin genes were amplified by PCR, cloned into pET16 plasmids, and introduced into *E. coli* by transformation. After induction of protein expression (1 mM isopropyl thiogalactoside, 3 h, 37 °C), cells were washed (150 mM NaCl) and lysed by sonication in buffer A (1M NaCl, 50 mM Tris-HCl (pH 8.0), 6M guanidine-HCl). Recombinant silaffins were isolated from the centrifuged supernatant (4 °C, 30 min, 10000 g) by Ni-NTA chromatography. Recombinant silaffin rSilC was subjected to an additional purification step by using cation exchange chromatography. Column eluates containing recombinant silaffins were dialyzed against ammonium acetate (50 mM), lyophyllized, and the residues were dissolved in H_2O. The yield was approximately 5 mg recombinant silaffin per liter of *E. coli* culture. Quantification of recombinant silaffins was performed after complete acid hydrolysis (6M HCl, 110 °C, 24 h) by reversed-phase HPLC of the phenylthiocarbamyl derivatives as described previously.[15b]

For titania formation, sodium phosphate/citrate buffer solution (20 μL of 500 mM) of the desired pH, TiBALDH (in H_2O; 20 μL of 2M), and H_2O (140 μL) were mixed and kept for 20 minutes at room temperature. Precipitation was initiated by adding recombinant silaffin (20 μL), and the reaction mixture was incubated for 10 minutes at room temperature. The precipitate was collected by centrifugation, washed three times each with H_2O (1 mL), and finally two times with methanol (1 mL). After the last centrifugation step, the precipitate was dried in a vacuum centrifuge overnight.

Silica precipitation was performed from freshly prepared silicic acid solutions (100 mM) that were adjusted to the desired pH by sodium phosphate/citrate buffer solution mixture (50 mM) as described previously.[15a] Silica quantification was performed by using the β-silicomolybdate assay.[17]

SEM was conducted with a field-emission gun microscope (Leo 1530 FEG SEM, Carl Zeiss SMT Ltd., Cambridge, UK) equipped with an EDX spectrometer (INCA EDS, Oxford Instruments, Bucks, UK). Precipitates were dried on a gold-coated aluminum SEM stub or silicon wafer. FIB-SEM was performed with a Nova 200 DBFIB FE-SEM equipped with a gallium ion FIB (FEI Company, Hillsboro, USA). TEM analysis was conducted with a JEOL 4000 EX instrument. HR-TEM analysis was conducted at an operating voltage of 400 kV. For TEM analysis, a drop of suspended precipitate was dried on a carbon-film-coated copper grid. Alternatively, the precipitate was resuspended in ethanol and ground with a mortar and pestle prior to drying.

Thermogravimetric analyses were conducted with a Netzsch 449C simultaneous thermal analyzer (Selb, Germany). Prior to analysis, samples were dried for 16 h at 65 °C.

Powder XRD was performed by using a PANalytical X-Pert Pro Alpha 1 diffractometer with an incident beam Johannsen monochromator, with 1/2° divergence slits, 0.04° soller slits, and an Xcelerator linear detector. The powder sample was loaded on a zero-background sample holder, and the measurement was performed over a 20–60° 2θ range by using a continuous scan with a 0.167° 2θ step size.

For polarized light microscopy, a Leica RDX microscope was used with the polarizer oriented 90° with respect to the analyzer.

Received: May 11, 2006
Revised: August 30, 2006
Published online: September 29, 2006

Keywords: biomimetic synthesis · crystal growth · proteins · sol–gel processes · titanium

[1] H. A. Lowenstam, S. Weiner, *On Biomineralization*, Oxford University Press, New York, **1989**.
[2] S. Mann, *Biomineralization*, Oxford University Press, Oxford, New York, **2001**.
[3] E. Bäuerlein, *Biomineralization*, Wiley-VCH, Weinheim, **2004**.
[4] A. H. Heuer, D. J. Fink, V. J. Laraia, J. L. Arias, P. D. Calvert, K. Kendall, G. L. Messing, J. Blackwell, P. C. Rieke, D. H. Thompson, A. P. Wheeler, A. Veis, A. I. Caplan, *Science* **1992**, *255*, 1098 – 1105.
[5] S. Mann, G. A. Ozin, *Nature* **1996**, *382*, 313 – 318.
[6] D. E. Morse, *Trends Biotechnol.* **1999**, *17*, 230 – 232.
[7] J. L. Sumerel, D. E. Morse in *Silicon Biomineralization* (Ed.: W. E. G. Müller), Springer, Berlin, **2003**, pp. 225 – 247.
[8] J. L. Sumerel, W. Yang, D. Kisailus, J. C. Weaver, J. H. Choi, D. E. Morse, *Chem. Mater.* **2003**, *15*, 4804 – 4809.
[9] D. Kisailus, M. Najarian, J. C. Weaver, D. E. Morse, *Adv. Mater.* **2005**, *17*, 1234 – 1239.
[10] P. Curnow, P. H. Bessette, D. Kisailus, M. M. Murr, P. S. Daugherty, D. E. Morse, *J. Am. Chem. Soc.* **2005**, *127*, 15749 – 15755.
[11] M. N. Tahir, P. Théato, W. E. G. Müller, H. C. Schröder, A. Janshoff, J. Zhang, J. Huth, W. Tremel, *Chem. Commun.* **2005**, 5533 – 5535.
[12] M. N. Tahir, P. Théato, W. E. G. Müller, H. C. Schröder, A. Borejko, S. Faiß, A. Janshoff, J. Huth, W. Tremel, *Chem. Commun.* **2004**, 2848 – 2849.
[13] T. Coradin, A. Coupé, J. Livage, *Colloids Surf. B* **2003**, 189 – 196.
[14] H. R. Luckarift, M. B. Dickerson, K. H. Sandhage, J. Spain, *Small* **2006**, *2*, 640 – 643.
[15] a) N. Kröger, R. Deutzmann, M. Sumper, *Science* **1999**, *286*, 1129 – 1132; b) N. Poulsen, M. Sumper, N. Kröger, *Proc. Natl. Acad. Sci. USA* **2003**, *100*, 12075 – 12080; c) N. Poulsen, N. Kröger, *J. Biol. Chem.* **2004**, *279*, 42993 – 42999.
[16] a) K. E. Cole, A. N. Ortiz, M. A. Schoonen, A. M. Valentine, *Chem. Mater.*, DOI: 10.1021cm060807b; b) R. R. Naik, M. O. Stone, *Mater. Today* **2005**, *8*, 18 – 26; c) M. J. Pender, L. A. Sowards, J. D. Hartgerink, M. O. Stone, R. R. Naik, *Nano Lett.* **2006**, *6*, 40 – 44; d) S. L. Sewell, D. W. Wright, *Chem. Mater.* **2006**, *18*, 3108 – 3113.
[17] R. K. Iler, *The Chemistry of Silica*, Wiley, New York, **1979**.
[18] S. V. Patwardhan, J. Clarson, C. C. Perry, *Chem. Commun.* **2005**, 1113 – 1121.
[19] P. J. Lopez, C. Gautier, J. Livage, T. Coradin, *Curr. Nanosci.* **2005**, 1, 73 – 83.
[20] U. Diebold, *Surf. Sci. Rep.* **2003**, *48*, 53 – 229.
[21] J. Ovenstone, P. J. Titler, R. Withnall, J. Silver, *J. Mater. Res.* **2002**, *17*, 2524 – 2531.
[22] A. R. Armstrong, G. Armstrong, J. Canales, P. G. Bruce, *Angew. Chem.* **2004**, *116*, 2336 – 2338; *Angew. Chem. Int. Ed.* **2004**, *43*, 2286 – 2288.
[23] M. Gopal, W. J. M. Chan, L. C. DeJonghe, *J. Mater. Sci.* **1997**, *32*, 6001 – 6008.
[24] J. Ovenstone, K. Yanagisawa, *Chem. Mater.* **1999**, *11*, 2770 – 2774.
[25] M. Wu, J. Long, A. Huang, Y. Luo, S. Feng, R. Xu, *Langmuir* **1999**, *15*, 8822 – 8825.
[26] S. T. Aruna, S. Tirosh, A. Zaban, *J. Mater. Chem.* **2000**, *10*, 2388 – 2391.
[27] W. P. Huang, X. H. Tang, Y. Q. Wang, Y. Koltypin, A. Gedanken, *Chem. Commun.* **2000**, 1415 – 1416.
[28] C. Wang, Z. X. Deng, Y. D. Li, *Inorg. Chem.* **2001**, *40*, 5210 – 5214.
[29] H. Yin, Y. Wada, T. Kitamura, S. Kambe, S. Murasawa, H. Mori, T. Sakata, S. Yanagida, *J. Mater. Chem.* **2001**, *11*, 1694 – 1703.
[30] W. W. So, S. B. Park, K. J. Kim, C. H. Shin, S. J. Moon, *J. Mater. Sci.* **2001**, *36*, 4299 – 4305.
[31] M. Andersson, L. Osterlund, S. Ljungstrom, A. Palmqvist, *J. Phys. Chem. B* **2002**, *106*, 10674 – 10679.
[32] D. B. Zhang, L. M. Qi, J. M. Ma, H. M. Cheng, *J. Mater. Chem.* **2002**, *12*, 3677 – 3680.
[33] S. Yin, R. X. Li, Q. L. He, T. Sato, *Mater. Chem. Phys.* **2002**, 75, 76 – 80.
[34] S. Yang, Y. Liu, Y. Guo, J. Zhao, H. Xu, Z. Wang *Mater. Chem. Phys.* **2003**, 77, 501 – 506.
[35] Z. L. Tang, J. Y. Zhang, Z. Cheng, Z. T. Zhang, *Mater. Chem. Phys.* **2003**, 77, 314 – 317.
[36] J. Yang, S. Mei, J. M. Ferreira, P. Norby, S. Quaresma, *J. Colloid Interface Sci.* **2005**, *283*, 102 – 106.
[37] L. Addadi, S. Raz, S. Weiner, *Adv. Mater.* **2003**, *15*, 959 – 970.
[38] J. Aizenberg, D. A. Muller, J. L. Grazul, D. R. Hamann, *Science* **2003**, *299*, 1205 – 1208.

